Quantitative phase separation in multiferroic $Bi_{0.88}Sm_{0.12}FeO_3$ ceramics via piezoresponse force microscopy

D. O. Alikin' , A. P. Turygin, J. Walker, T. Rojac, V. V. Shvartsman, V. Ya. Shur, and A. L. Kholkin

Quantitative phase separation in multiferroic $Bi_{0.88}Sm_{0.12}FeO_3$ ceramics via piezoresponse force microscopy

D. O. Alikin,[1,a)] A. P. Turygin,[1] J. Walker,[2] T. Rojac,[2] V. V. Shvartsman,[3] V. Ya. Shur,[1] and A. L. Kholkin[1,4]

[1]*Institute of Natural Sciences, Ural Federal University, 620000 Ekaterinburg, Russia*
[2]*Electronic Ceramics Department, Jozef Stefan Institute, 1000 Ljubljana, Slovenia*
[3]*Institute for Materials Science, University of Duisburg Essen, D 45141, Essen, Germany*
[4]*Department of Physics & CICECO Aveiro Institute of Materials, University of Aveiro, 3810 193 Aveiro, Portugal*

$BiFeO_3$ (BFO) is a classical multiferroic material with both ferroelectric and magnetic ordering at room temperature. Doping of this material with rare-earth oxides was found to be an efficient way to enhance the otherwise low piezoelectric response of unmodified BFO ceramics. In this work, we studied two types of bulk Sm-modified BFO ceramics with compositions close to the morphotropic phase boundary (MPB) prepared by different solid-state processing methods. In both samples, coexistence of polar $R3c$ and antipolar P_{bam} phases was detected by conventional X-ray diffraction (XRD); the non-polar P_{nma} or P_{bnm} phase also has potential to be present due to the compositional proximity to the polar-to-non-polar phase boundary. Two approaches to separate the phases based on the piezoresponse force microscopy measurements have been proposed. The obtained fractions of the polar and non-polar/anti-polar phases were close to those determined by quantitative XRD analysis. The results thus reveal a useful method for quantitative determination of the phase composition in multi-phase ceramic systems, including the technologically most important MPB systems. © 2015 AIP Publishing LLC. [http://dx.doi.org/10.1063/1.4927812]

I. INTRODUCTION

Existence of a morphotropic phase boundary (MPB) in ferroelectric materials leads to the important improvement of a variety of bulk properties, such as dielectric permittivity, piezoelectric coefficients, and remanent polarization.[1] $BiFeO_3$ (BFO), which has attracted much research attention due to coexistence of ferroelectric and magnetic ordering,[2–5] is an important lead-free piezoelectric material and it is considered as a replacement for conventional lead zirconate titanate ceramics due to severe restrictions of using toxic lead in electronic components.[6,7] It has been recently demonstrated that a polar-to-non-polar phase transition with associated enhancements in the electromechanical response can be induced by the isovalent substitution of Bi^{3+} with rare-earth elements, such as La^{3+} and Sm^{3+}.[8–12] The structure of BFO substituted with rare-earth compositions has been extensively studied by integral methods, such as Rietveld refinement of X-ray Diffraction (XRD) patterns, and additional methods[13–15] and only a few reports by local methods, such as transmission electron microscopy, have been published.[15–18] The phases that appear in the close proximity to the MPB are polar $R3c$, non-polar P_{nma}, and antipolar P_{bam} phases.[15] Fractions of these phases and their distribution, which may strongly affect properties in the MPB systems, are dependent on chemical homogeneity and sintering conditions, such as temperature.[18] It is thus of interest to develop reliable methods for the analysis of these phases both from the perspective of structure-property relations in these materials and to further investigate their possible use as lead-free piezoelectric materials. Unfortunately, existing methods to analyze local distribution of these phases are quite limited, despite the fact that they are important for the functional behavior of the ceramics. It is also known that XRD methods are largely inaccurate for determining different oxygen octahedral tilts, something which may be vital for distinguishing between distorted perovskite phases with similar lattice parameters[19] and thus, additional methods for distinguishing between perovskite phases at an MPB are desirable. Additionally, powder XRD of polycrystalline materials does not provide information regarding the spatial distribution of the phases within the ceramic; thus, additional valuable information can be obtained from local piezoresponse force microscopy (PFM) measurement techniques.

In this paper, we consider two approaches to measure the spatial distribution of the polar and non-polar/anti-polar phases at the local scale by PFM and estimate the volume fraction of each phase in bulk Sm-doped BFO ceramics with compositions near the MPB. The proposed approaches assist with clarification of the difference between ceramics prepared by a conventional solid state sintering technique and a solid state sintering technique with additional mechanochemical activation. Samples prepared by both techniques are of particular interest as they have recently been shown to exhibit good ferroelectric and electromechanical responses under high electric field.[18]

II. EXPERIMENTAL

The investigated 1-mm-thick pellets of ceramic samples of $Bi_{0.88}Sm_{0.12}FeO_3$ (Sm-BFO) were prepared by two

a)Author to whom correspondence should be addressed. Electronic mail: denis.alikin@urfu.ru

different methods: conventional solid state synthesis (non-activated sample) and solid state synthesis with additional mechanochemical activation for 40 h (activated sample). The details of both synthesis procedures have been published elsewhere.[18] The XRD patterns of the ceramics were recorded using a Bruker D8 Discover diffractometer, in a 10–90° 2θ range with a step of 0.04° and an acquisition speed of 1.5°min[−1]. Analysis was carried out on ceramics sintered at 820 °C and 800 °C with non-activated and activated processes, respectively (sintering time 4 h). Rietveld refinements were performed using TOPAZ R software package (Version 2.1, 2003, Coelho software). The peak shape was refined using a Voigt function, the background was refined with a linear function, and the peak intensities, shapes, and scale factors were fitted before refining the unit cell parameters. The ceramics showed coexistence of two phases fitted with ICSD cards: polar rhombohedral $R3c$ phase (ICSD#15299) and anti-polar orthorhombic P_{bam} phase (ICSD#162895) (Table I). The non-polar orthorhombic P_{nma}/P_{bnm} phase (ICSD#160460) was observed only in non-activated samples at lower sintering temperatures.[18] Vector piezoresponse force microscopy (VPFM) was applied for the local study of the phase coexistence and measurements of their distribution. The measurements were performed with a scanning probe microscope MFP-3D (Asylum Research, USA) using probes DPE-16 with platinum conductive coating (Mikromasch, Estonia) having radius of curvature ∼40 nm and resonance frequency 170 kHz (spring constant 42 N/m). 10 V AC voltage with frequency 20 kHz (far from the contact resonance) was applied to the probes for out-of-plane and in-plane PFM imaging. Spatial distribution of $Y = R \sin\Theta$ piezoresponse signal (where R — amplitude, θ is the phase) was detected by internal lock-in amplifier and represented as a PFM image.

III. RESULTS AND DISCUSSION

The XRD patterns from both the non-activated and the activated samples (Fig. 1) are indexed with a rhombohedral phase, with space group $R3c$ (ICSD#15299), approximately isostructural to BiFeO$_3$. The $R3c$ peaks of both ceramics are shifted to higher 2θ values, relative to unmodified BiFeO$_3$ (pattern not shown), which is in agreement with the unit cell reduction which occurs as a function of the increased inclusion of the smaller ionic radius Sm^{3+} cation at the A site of
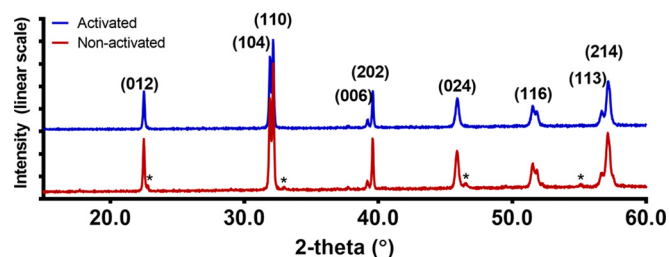

FIG. 1. X-ray diffraction patterns for samples prepared by conventional solid state synthesis (non-activated) and solid state synthesis with additional mechanochemical activation (activated). Rhombohedral peaks belonging to the $R3c$ space group are indexed, and * (star) indicates distinguishable peaks associated with orthorhombic P_{bam} anti-polar phase.

the perovskite, substituting for the larger ionic radius Bi^{3+}.[18] For the XRD patterns of these two samples, the anti-polar orthorhombic $Pbam$ phase (ICSD#162895) was also required for fitting of the patterns with Rietveld refinement. The star (*) in Fig. 1 indicates the peaks from the P_{bam} phase, which are visible. From Fig. 1, it appears as though the P_{bam} phase peaks are only visible in the non-activated ceramics, however, it is important to note that the highest intensity P_{bam} peak (122) is overlapped by the shifted R3c (110) peak. For this reason, the phase compositions as determined by Rietveld refinement of the XRD patterns (Table I) should be confirmed with additional analysis.

The approach for differentiating between the different phases in Sm-BFO ceramics with the PFM technique is based on the apparent absence of a piezoresponse in non-polar and anti-polar phases, because they are not piezoelectric. For the purposes of the phase analysis performed by PFM discussed in the following, the non-polar orthorhombic phase P_{nma} or P_{bnm} was considered as possibly present, despite its absence from the XRD patterns (Fig. 1).

In order to determine the area fraction of the phases with no piezoresponse in ceramics with randomly oriented grains, it is necessary to measure the piezoelectric effect in three orthogonal spatial directions and to determine the direction and value of the spontaneous polarization vector. While this can be performed,[20] the task is rather complicated, as for such an analysis, the sample needs to be rotated by 90° around the axis normal to the sample surface (to obtain both x- and y-components of the spontaneous polarization). At the same time, it is known that already two PFM signals contain information sufficient to reconstruct all the three components of the spontaneous polarization. Due to cantilever buckling, the vertical deflection provides information not only about the out-of-plane component of the polarization vector (Fig. 2(a)) but also contains contribution related to the in-plane polarization parallel to the cantilever long axis (Fig. 2(b)).[21] Information about the third component of polarization (in-plane, perpendicular to the cantilever) can be obtained from the twisting motion of the cantilever (Fig. 2(c)). Therefore, only two PFM signals (vertical and one lateral) are sufficient to prove the presence (or absence) of the piezoelectric phase in selected grains.

VPFM images of the non-activated and activated ceramics of Sm-BFO demonstrate the coexistence of the piezoelectric regions with different values of the piezoresponse

TABLE I. Fractions of the polar and anti-polar/non-polar phases obtained by different experimental methods.

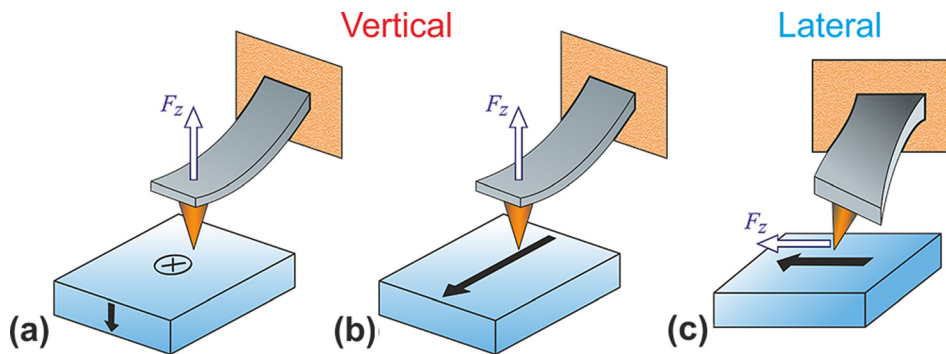| Method	Non-activated ceramics		Activated ceramics	
	Polar phase	Anti-polar/ nonpolar phase	Polar phase	Anti-polar/ nonpolar phase
XRD	84	16	89	11
VPFM leveling by Gauss approximation	72	28	70	30
VPFM leveling by noise histogram	83	17	94	6

FIG. 2. Tip interaction with domains oriented in different directions and corresponding signals: (a) and (b) vertical and (c) lateral.

and areas without piezoresponse in both out-of-plane and in-plane images (Fig. 3). The separation of the polar and anti-polar/non-polar phases was based on the analysis of histograms of PFM signal, which includes information about the distribution of piezoelectrically active and non-active areas, shown as insets in Fig. 3. In all cases, a single peak with a broad distribution of color contrast was observed.

The analysis was performed in the frame of two different approaches. In both, we assumed that the area of the phase without a piezoresponse had a value near the average noise signal in the histogram (which have been measured without contacting the sample surface).

The first approach was similar that used by the authors of Refs. 22 24. The obtained histograms were fitted by three Gaussian functions, assuming that three different polarization states could be separated by their piezoresponse signal level. These polarization states are related to the polar phases with opposite direction of spontaneous polarization (D_{eff}^+, D_{eff}^-)

and anti-polar/non-polar phases (D_{eff}^0). The D_{eff}^0 signal value has been chosen near the average position. The interceptions of Gaussian functions were used for the phase separation (Figs. 4(b) and 4(d)). The interception of Gaussian with D_{eff}^- and D_{eff}^0 gives the minimum value of the piezoresponse signal, which can be interpreted as being related to the polar phase, while the interception of D_{eff}^+ and D_{eff}^0 gives the maximum value. These values were used for the image binarization. The blue mask overlapped with the PFM image demonstrates the distribution of the area of the phase without piezoresponse.

In the second approach, the half-width of the noise peak in the histogram was chosen as the level for the binarization (Fig. 4).

In both approaches, the separated area, corresponding to the phase with no piezoresponse, has different distribution in the out-of-plane and in-plane PFM images. This can be attributed (as have been mentioned before) to the orientation of
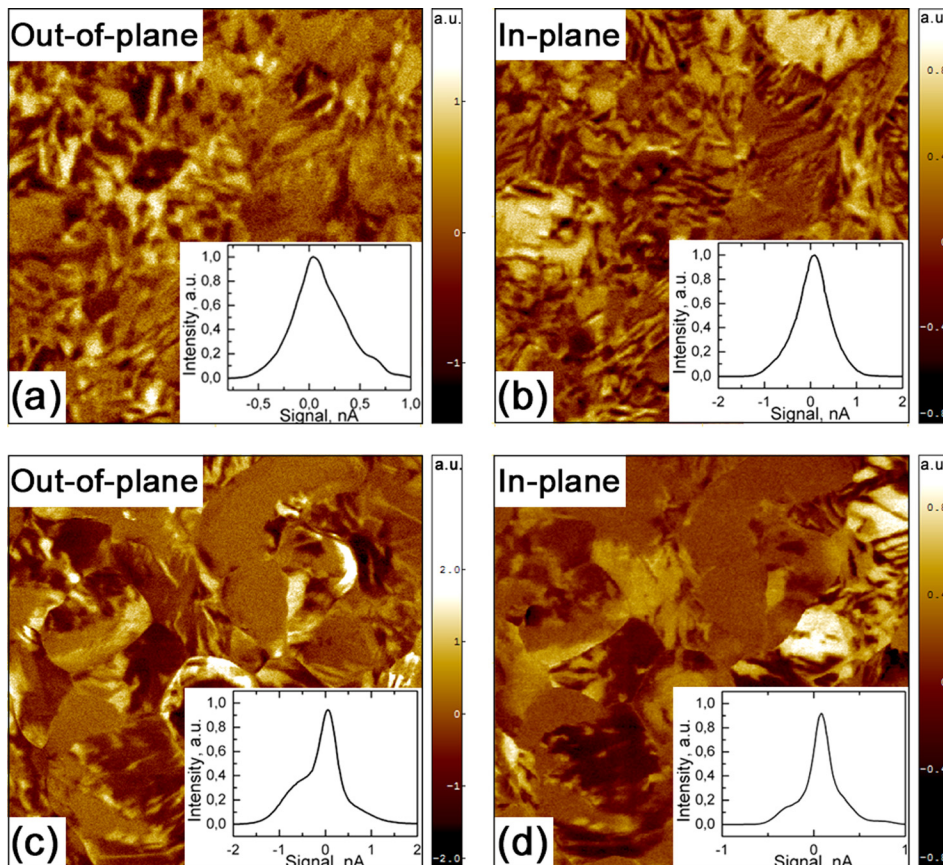

FIG. 3. PFM images ($10 \times 10\,\mu$m) and corresponding histograms of the (a) and (b) activated and (c) and (d) non activated samples.
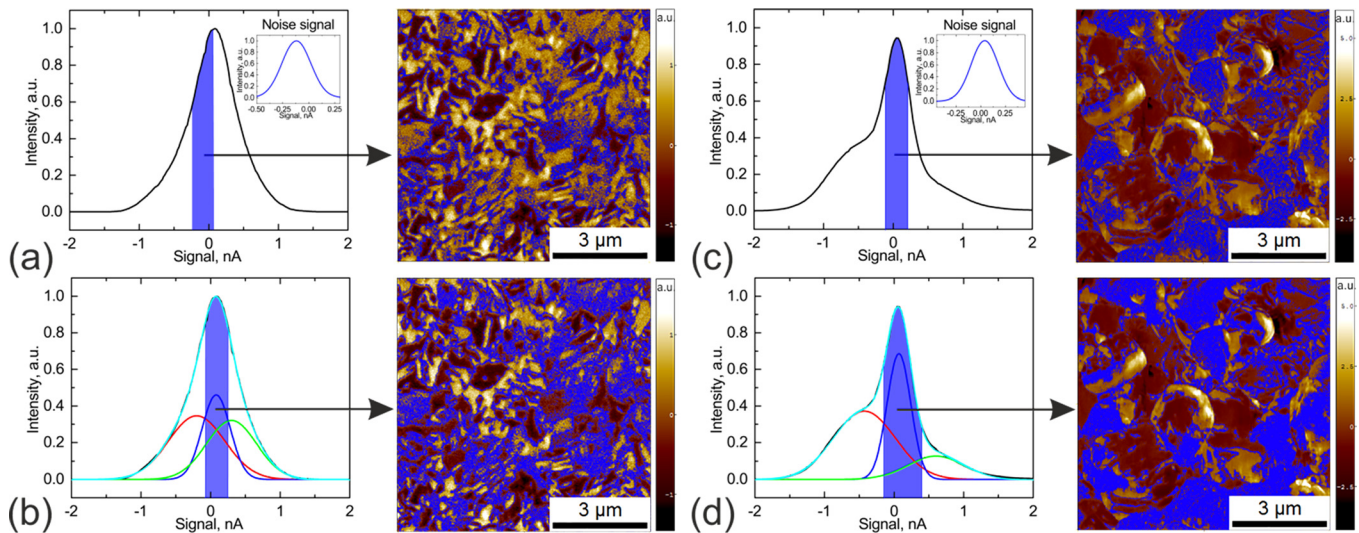
FIG. 4. Extraction of the area with absence of the piezoresponse in (a) and (b) activated and (c) and (d) non activated samples by (a) and (c) comparison with noise signal and by (b) and (d) approximation of the histograms with three Gaussians.

some grains in the ceramics in a direction that minimizes the piezoresponse either in the out-of-plane or in-plane images. Here, we used the calculation of the intersection of the area without piezoresponse in the out-of-plane and in-plane images to extract the area of anti-polar/non-polar phases (Fig. 5). The fractions of the phases were then extracted as ratios of the areas of the intersections with the whole area of scans.

It can be argued that the obtained values of the relative fractions of polar and non-polar phases refer to the surface (rather than bulk) effect. However, it is known that PFM effectively probes the depth down to a few microns[25] (i.e., comparable to the average grain size in the studied ceramics) so it can be said that obtained fractions are characteristic of the ceramics bulk. Accuracy of the method was estimated to be around 5% based on the averaging of 10 PFM scans with 15 20 grains each. For the ceramics with much bigger average grain size, the significant increase in the experimental error can be observed. Along with increase in the scan size due to necessity to include enough for averaging number of grains and as consequence, increase in scanning duration (about 1 2 h for the scan) proposed method becomes sufficiently non-effective.

Comparison of the images in Fig. 4 clearly demonstrates the difference in the selected area for the two

approaches. The phase fractions measured by PFM, of the polar and anti-polar/non-polar phases, generally correlate well with those obtained by the XRD analysis (Table I). The second PFM approach, which used the noise level determined from the histogram's semi-width, resulted in phase fraction values closer to those determined by the XRD analysis, as compared to the first PFM approach described (Table I). The differences in the phase fractions determined by the VPFM and XRD methods can be attributed to

(i)   difference between the volume fraction (obtained by XRD) and surface fractions (acquired by VPFM) due to inhomogeneity of the phase distribution in bulk in different parts of the sample,
(ii) not a large enough surface area scan size for comprehensive statistical analysis appeared as result of time consuming demands,
(iii) the fact that the XRD patterns were taken from the crushed pellets, in which the strain states of the resulting powder could be different from those of the sintered pellets, used for PFM, where the grains were elastically interconnected. Additionally, the XRD patterns of the three constituent phases contain considerable peak
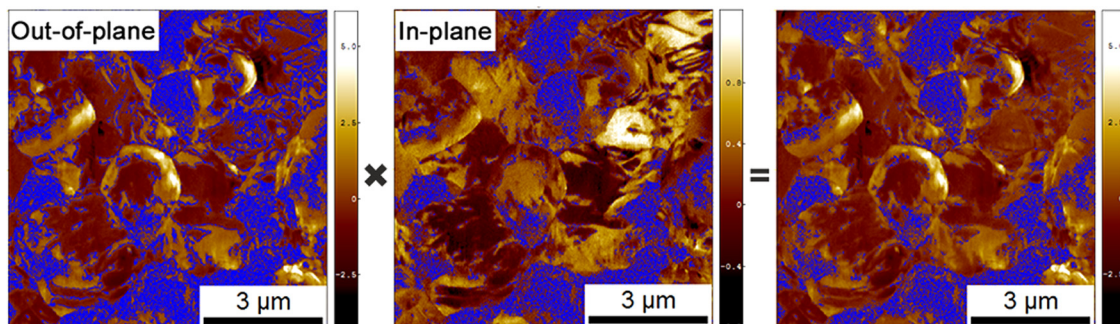

FIG. 5. Areas with the absence of piezosignal in out of plane image, in plane image, and their interception corresponding to the distribution of the anti polar/ non polar phase (by example of second approach).

overlap, which can lead to errors during refinements.[26] XRD is largely insensitive to oxygen positions; hence, structurally similar perovskite phases can be difficult to identify without the use of additional methods.[15,27]

For better separation of the phases, local poling or voltage-spectroscopy-based methods can be used; however, these methods can give other errors caused by the electric field induced transitions and switching between non-polar and polar phases during experiments.

By comparing the results of XRD and VPFM (noise method), we can see that the additional mechanochemical activation results in a minor reduction in the fraction of the anti-polar phase (Table I). This may be related to the formation of nanosize grains of P_{bam} phase within $R3c$ rhombohedral grains, as has been recently observed by TEM, and/or to the difference in chemical homogeneity observed between the two ceramics, which results from the difference in the reaction pathways.[18] The phase composition of the activated and non-activated samples observed by VPFM using leveling by Gaussian approximation is similar; however, the absolute values of polar phase were underestimated in this case. Better description of the polar fractions is given by VPFM with leveling by noise histogram, where the results are approximately within the anticipated ± 5 wt. % error of the XRD values. The results are in general consistent with the recent TEM analysis, which determined the arrangement of both polar and anti-polar phases within individual grains.

IV. CONCLUSIONS

Here, we studied two differently processed Sm-modified BFO ceramics using PFM. Two approaches were used to separate the coexisting polar and non-polar/anti-polar phases: (i) approximation of the resulting PFM histograms by Gaussians and (ii) comparison of the PFM images with the level of noise. The second proposed approach gives values of the fractions of the polar and anti-polar/non-polar phases which better matching to the values evaluated by XRD of the polycrystalline powders of the same ceramics. The differences in the phase fractions derived by these methods can be attributed to the inhomogeneous phase distributions and intrinsic features of the PFM imaging. Thus, the PFM techniques can be successfully used for local phase analysis of the ferroelectric samples and provided a tool for the study of the influence of the processing methods on the phase coexistence in Sm-modified BFO.

ACKNOWLEDGMENTS

[1]B. Jaffe, W. R. Cook, and H. L. Jaffe, *Piezoelectric Ceramics* (Academic Press, New York, 1971).
[2]J. Rodel, W. Jo, K. T. P. Seifert, E. M. Anton, T. Granzow, and D. Damjanovic, J. Am. Ceram. Soc. **92**, 1153 (2009).
[3]E. Aksel and J. L. Jones, Sensors **10**, 1935 (2010).
[4]T. R. Shrout and S. J. Zhang, J. Electroceram. **19**, 185 (2007).
[5]G. Catalan and J. F. Scott, Adv. Mater. **21**, 2463 (2009).
[6]European Union, in *2002/96/EC*, 2003.
[7]European Union, in *Directive 2002/95/EC*, 2003.
[8]S. Fujino, M. Murakami, V. Anbusathaiah, S. H. Lim, V. Nagarajan, C. J. Fennie, M. Wuttig, L. Salamanca Riba, and I. Takeuchi, Appl. Phys. Lett. **92**, 202904 (2008).
[9]I. O. Troyanchuk, D. V. Karpinsky, M. V. Bushinsky, V. A. Khomchenko, G. N. Kakazei, J. P. Araujo, M. Tovar, V. Sikolenko, V. Efimov, and A. L. Kholkin, Phys. Rev. B **83**, 054109 (2011).
[10]D. V. Karpinsky, I. O. Troyanchuk, V. Sikolenko, V. Efimov, and A. L. Kholkin, J. Appl. Phys. **113**, 187218 (2013).
[11]D. V. Karpinsky, I. O. Troyanchuk, M. Tovar, V. Sikolenko, V. Efimov, and A. L. Kholkin, J. Alloys Compd. **555**, 101 (2013).
[12]V. A. Khomchenko, J. A. Paixao, V. V. Shvartsman, P. Borisov, W. Kleemann, D. V. Karpinsky, and A. L. Kholkin, Scr. Mater. **62**, 238 (2010).
[13]D. Kan, L. Pálová, V. Anbusathaiah, C. J. Cheng, S. Fujino, V. Nagarajan, K. M. Rabe, and I. Takeuchi, Adv. Funct. Mater. **20**, 1108 (2010).
[14]I. O. Troyanchuk, D. V. Karpinsky, M. V. Bushinsky, O. S. Mantytskaya, N. V. Tereshko, and V. N. Shut, J. Am. Ceram. Soc. **94**, 4502 (2011).
[15]S. Karimi, I. M. Reaney, Y. Han, J. Pokorny, and I. Sterianou, J. Mater. Sci. **44**, 5102 5112 (2009).
[16]A. Srivastava, H. K. Singh, V. P. S. Awana, and O. N. Srivastava, J. Alloys Compd. **552**, 336 344. (2013).
[17]C. J. Cheng, A. Y. Borisevich, D. Kan, I. Takeuchi, and V. Nagarajan, Chem. Mater. **22**, 2588 2596 (2010).
[18]J. Walker, P. Bryant, V. Kurusingal, C. Sorrell, D. Kuscer, G. Drazic, A. Bencan, V. Nagarajan, and T. Rojac, Acta Mater. **83**, 149 (2015).
[19]C. J. Cheng, D. Kan, S. H. Lim, W. R. McKenzie, P. R. Munroe, L. G. Salamanca Riba, R. L. Withers, I. Takeuchi, and V. Nagarajan, Phys. Rev. B **80**, 014109 (2009).
[20]S. V. Kalinin, B. J. Rodriguez, S. Jesse, J. Shin, A. P. Baddorf, P. Gupta, H. Jain, D. B. Williams, and A. Gruverman, Microsc. Microanal. **12**, 206 (2006).
[21]E. Soergel, J. Phys. D: Appl. Phys. **44**, 464003 (2011).
[22]A. Wu, P. M. Vilarinho, V. V. Shvartsman, G. Suchaneck, and A. L. Kholkin, Nanotechnology **16**, 2587 (2005).
[23]V. V. Shvartsman and A. L. Kholkin, J. Appl. Phys. **108**, 042007 (2010).
[24]V. V. Shvartsman and A. L. Kholkin, Phys. Rev. B **69**, 014102 (2004).
[25]F. Johann, Y. J. Ying, T. Jungk, A. Hoffmann, C. L. Sones, R. W. Eason, S. Mailis, and E. Soergel, Appl. Phys. Lett. **94**, 172904 (2009).
[26]H. Rietveld, J. Appl. Crystallogr. **2**, 65 (1969).
[27]I. M. Reaney, D. I. Woodward, and C. A. Randall, J. Am. Ceram. Soc. **94**, 2242 (2011).